Original Article

Development of high-capacity $Ni(OH)_2$ electrode using granulation process

Kazuya Nishimura (GIGACELL Battery Center, Rolling Stock Company, Kawasaki Heavy Industries, Ltd., nishimura_kazuya@khi.co.jp)
Tomoaki Takasaki (GIGACELL Battery Center, Rolling Stock Company, Kawasaki Heavy Industries, Ltd., takasaki_t@khi.co.jp)
Tetsuo Sakai (Research Institute for Ubiquitous Energy Devices, National Institute of Advanced Industrial Science and Technology, sakai-tetsuo@aist.go.jp)

Abstract

A large-size battery for future industrial applications requires a higher capacity and longer cycle-life than that for the consumer applications. The $Ni(OH)_2$ was granulated with conductive and binder materials, and the granulated particles were sandwiched between two nickel-foam pieces to form a plate-like positive electrode. The capacity was estimated to be 54 mAh/cm^2, which was higher than that of the conventional paste-type one (36 mAh/cm^2), loading the $Ni(OH)_2$ slurry on the nickel-foam substrate. In this electrode structure, the granulated particles can be easily maintained on the substrate in the electrolyte. The battery test using the granulated $Ni(OH)_2$ electrode showed that the cycle-life performance could be improved by increasing the amount of separator compression. The high compression suppressed the electrode expansion by electrolyte absorption, which causes electrolyte loss during the charge and discharge processes.

Key words

granulated particle, nickel hydroxide, nickel-metal hydride battery, secondary battery, industrial application

1. Introduction

After the industrial revolution, mankind invented a method to get electrical energy from fossil fuels. The energy consumption has exponentially increased by the shift to industrialization with mass-production and mass-consumption and the information-oriented society with the development of the IT technique, causing various environmental problems such as limited fossil fuel resources, air pollution and global warming.

In Japan, new technologies such as alternative energy and energy savings have attracted much interest by the global deployment of a new fiscal policy called the "Green New Deal". In the near future, the ratio of power generation using a renewable energy, such as solar and wind, would be increased. Moreover, the energy savings using a battery is promoted not only for cars (Sakai, 2010; Sakai and Sato, 2003), but also for public transportation such as trains (Nishimura and Tsutsumi, 2007; Tsutsumi, 2008; Tsutsumi and Matsumura, 2009; Yamazaki et al., 2010; Ogura et al., 2010). A large battery with a high-capacity and long cycle-life is indispensable to absorb the load fluctuations of generation and railways. In order to meet this requirement, the development of a higher-capacity electrode than the conventional one would be one of the effective ways.

For industrial applications, a number of single cells are stacked to assemble a high voltage battery. A difference in the state of charge gradually increases during the charge and discharge cycles, and some cells could be overcharged and overdischarged. For the conventional positive electrode containing a CoOOH conductive material, the overdischarge causes degradation of the battery performance as well as disruption of the CoOOH conductive network (Takasaki et al., 2013). In addition, cobalt is an expensive rare metal, and its price has often noticeably fluctuated. The securing of a stable supply is a serious concern. Therefore, the Co-free $Ni(OH)_2$ electrode is an important subject for the Ni-MH battery.

Furthermore, as for the battery for industrial applications, the long-term durability of 15 years is required. In this case, it is necessary to increase the electrolyte quantity compared to a consumer battery to prevent electrolyte loss. However, for the conventional paste-type electrode, loading the $Ni(OH)_2$ slurry on the nickel-foam substrate, if there is too much electrolyte, the $Ni(OH)_2$ particles would be easily separated from the nickel-foam substrate. A binder material, which exhibits a good adhesion, is necessary.

In this study, a high-capacity positive electrode with the long-term durability was prepared by granulating the $Ni(OH)_2$ with conductive and binder materials. The battery performances dependent on this addition were investigated and the optimum addition was investigated. A small-sized test cell consisting of a structure that is equivalent to a large-sized Ni-MH battery, called the GIGACELL (Nishimura and Tsutsumi, 2007; Tsutsumi, 2008; Tsutsumi and Matsumura, 2009; Yamazaki et al., 2010; Ogura et al., 2010), was constructed, and the contact pressure between the electrode and separator was measured and the correlation among the electrode-expansion, the electrolyte-loss and cycle-life performance was investigated.

2. Experimental

As the positive material, spherical $Ni(OH)_2$ particles with an approximate 10 μm size were used. An oxidation-resistant carbon black (ORCB) and Ni-plated carbon fiber (Ni-CF) were used as the conductive materials. In this experiment, the

$Co(OH)_2$ was not added as the conductive agent. The ORCB was prepared by annealing carbon black at approximately 2500 K in an N_2 atmosphere. The heating time was 3 hours. Ethylene vinyl acetate (EVA), which exhibits a good oxidation-resistance, is alkali-proof and has a good binding strength, was also used.

The ORCB, Ni-CF and EVA were added to a xylene solvent at the weight ratio of 1:1:1, then stirred while heating to 333 K to obtain a uniform slurry. The positive granulated particles were formed by adding $Ni(OH)_2$ powder, and mixing it with a high-speed-mixer LFS-2 (Earthtechnica Co., Ltd., Japan) while heating. The mixing time was 10 minutes. In addition, the $MmNi_{3.7}Co_{0.7}Mn_{0.3}Al_{0.3}$ alloy particles with an approximate 50 μm size was used as the negative material, and negative granulated particles were made using a manufacturing method equivalent to the positive one.

The granulated particles were molded as electrodes for the battery test by maintaining them at 333 K for 10 minutes while compacting them by at 6 MPa after sandwiched between two pieces of nickel-foam with 0.04 g/cm^2 of the weight per area. The GIGACELL-type single cells (Nishimura and Tsutsumi, 2007; Tsutsumi, 2008; Tsutsumi and Matsumura, 2009; Yamazaki et al., 2010; Ogura et al., 2010) with a 15 Ah rating were constructed using the granulated electrodes. Inside the cells, pre-formed stripes of positive and negative electrodes are inserted into the respective sides of the pleat-folded separator. The separator thickness was 0.4 mm. The electrolyte was 6 mol/L KOH.

As a probe to measure the pressure change between the electrode and separator during the charge/discharge process, three small-sized LM-100KA-P load-cells (Kyowa Electronic Instruments Co., Ltd., Japan) were sandwiched between two pieces of stainless steel boards with the same size as the electrode and fixed in place. The entire probe was sealed in a plastic bag and inserted into a separator with the electrodes. The total of the measured values of the 3 load-cells was divided by the electrode area to obtain the pressure (kgf/cm^2). An autograph AG-100kNG (Shimadzu Corporation) was used for measuring the repulsive force during the separator compression.

3. Results and discussion

3.1 Electrode preparation and performance

The obtained granulated particles were shifted, and the particles with an approximate 3mm size were sorted as shown in Figure 1. The ORCB and Ni-CF dispersed around the $Ni(OH)_2$ particles could contribute to improving the electrical conductivity, while the EVA plays a role to maintain the shape of the granulated particles as binder.

In the electrode molding process, the granulated particles were sandwiched between two nickel-foam pieces and pressed while heating as shown in Figure 2(a). Figure 2(b) shows a photograph of the molded electrodes. The thickness of the electrodes was approximately 1.2 mm, and the density of the granulated particles was approximately 1.8-2.0 g/cm^3. In addition, it was difficult to mold the electrode at room temperature because the EVA does not work as an adhesive at this temperature.

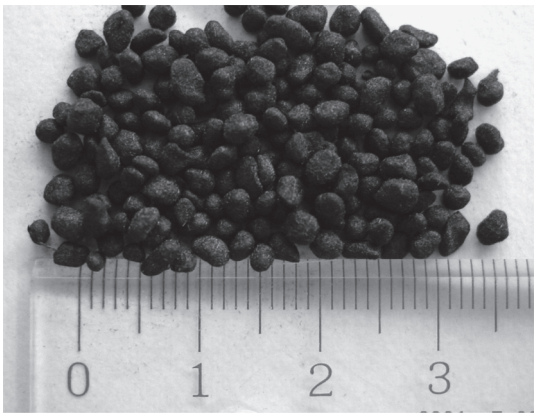

Figure 1: Photograph of the granulated $Ni(OH)_2$ particles

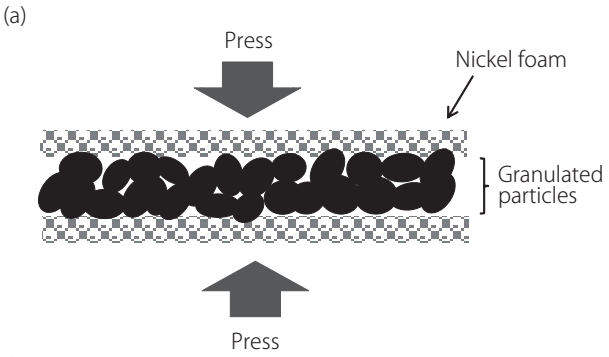

Figure 2: (a) Schematic view of electrode molding process, (b) granulated particles sandwiched between nickel foams and pressed while heating at 333 K

Table 1 shows the energy density of the granulated electrode compared to that of the various conventional sintered

Table1: Energy density for various electrodes

Electrode type	Energy density		Electrode thickness
	mAh/cm^2	mAh/cm^3	mm
Granulated particle	54	450	1.2
Ni-foam	36	600	0.6
Sintered	20	400	0.5

Table 2: The weight ratio of active materials and additives, resistance of electrode and high-rate performance

							Discharge capacity (mAh/g)		
	No.	$Ni(OH)_2$	EVA	CB	PAN	Resistance (Ω)	0.1 C	1 C	5 C
Positive electrode	#1	100	10	10	10	7.0	230	195	52
	#2	100	5	5	5	8.2	248	230	69
	#3	100	2.5	2.5	2.5	103	151	38	1
							Discharge capacity (mAh/g)		
	No.	MH	EVA	CB	PAN	Resistance (Ω)	0.1C	1 C	5 C
Negative electrode	#1	100	2.5	2.5	2.5	0.27	270	244	55
	#2	100	1.25	1.25	1.25	0.25	236	217	21

(Fleischer, 1948; Falk and Salkind, 1969; Ng and Schneider, 1986) and paste-type (Oshitani et al., 1989; Yao et al., 2007) ones. The capacity per unit volume (mAh/cm3) was comparable or greater than that of the sintered electrode, while the capacity per unit area (mAh/cm^2), which was estimated by dividing the capacity per unit volume in the electrode thickness, was 1.5-2 times greater than the paste-type one using Ni-foam substrate.

As shown in Table 2, the electrical resistance of the positive electrode decreased with the increasing conductive additives. The conductive materials would improve the low electrical conductivity of the $Ni(OH)_2$. However, the high-rate discharge performances of electrode p#1, which exhibited the best electrical conductivity, were inferior to those of electrode p#2. This result indicates that a large amount of the conductive material would reduce the $Ni(OH)_2$/electrolyte interface, and prevent the electrochemical reaction by ionic diffusion. The high-rate performances of electrode p#3 suggest that the electrical conductivity was not sufficiently improved even if the $Ni(OH)_2$/electrolyte interface is sufficient. The amount of additives for electrode p#2 is the most suitable for improving the electrode performance.

For the negative electrode, two electrodes were tested. Electrode n#1 with higher amount of additives exhibited the better performance. The higher amount of EVA would improve the adhesion of the alloy particles to the nickel-foam substrate. The amount of additives in the negative electrodes was lower than that of the positive ones. This would be related to the good metallic conductivity of the negative alloy compared to the $Ni(OH)_2$. In the following battery tests, electrodes p#2 and n#1 were used.

3.2 Pressure variation between the electrode and separator

The test batteries, which had a structure equivalent to the GIGACELL (Nishimura and Tsutsumi, 2007; Tsutsumi, 2008; Tsutsumi and Matsumura, 2009; Yamazaki et al., 2010; Ogura et al., 2010), were constructed using electrodes p#2 and n#1 as shown in Figure 3. The pressure upon a unit area between

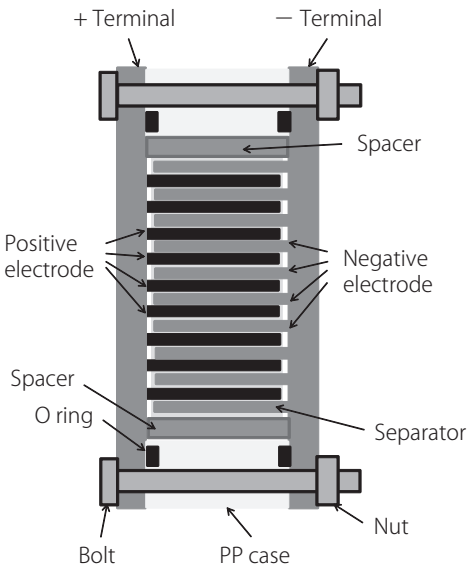

Figure 3: Schematic view of GIGACELL-type test battery

the electrode and separator was monitored using the inserted load-cells. The value of separator thickness was designed to be 0.4 mm, which is equal to the original thickness.

Figure 4 shows the cycle-dependent battery performances, namely, the Ah-efficiency, average discharge voltage and voltage at the end of charging. The initial performances were maintained to the 100th cycle. After 130 cycles, the Ah efficiency decreased, and a discharge-voltage reduction and charge-voltage increase were also observed.

Figure 5 shows the pressure variation during the charge and discharge processes at the 41th and 130th cycles. At the 41th cycle, the pressure decreased during the initial step of the charging process, and increased with the increasing charging. At the beginning of the discharge process, the pressure decreased, then increased from the middle of the discharge again. The pressure variation exhibited a similar behavior at the 130th cycle, but the pressure level rose in comparison to the value at the 41th cycle. The pressure value at the 130th cycle was in the range of 1.5-2.4 kgf/cm^2. This value

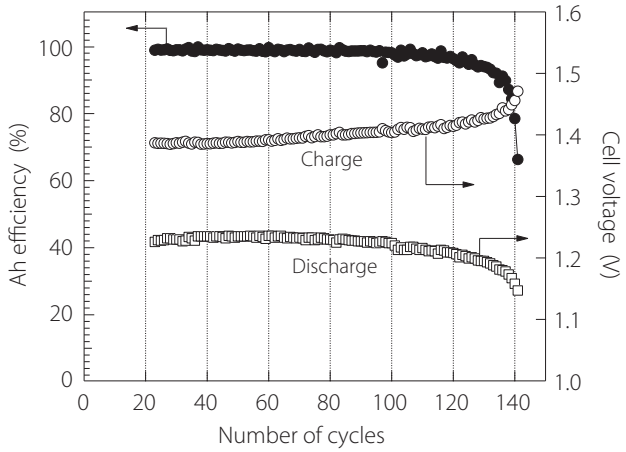

Figure 4: Cycle-life performance of the test battery without separator compression

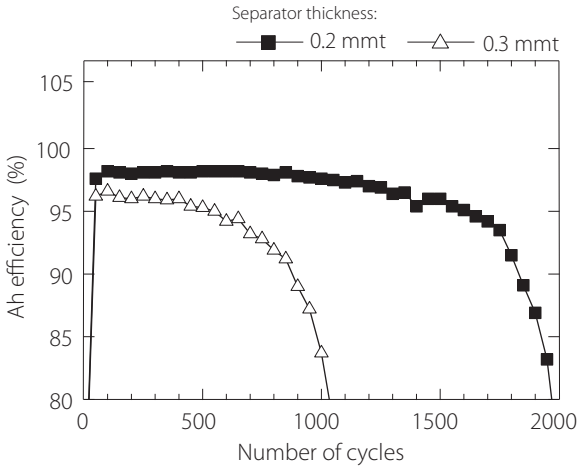

Figure 6: Cycle-life performance with the separator compression (a) 0.2 mm as the designed thickness, (b) 0.3 mm

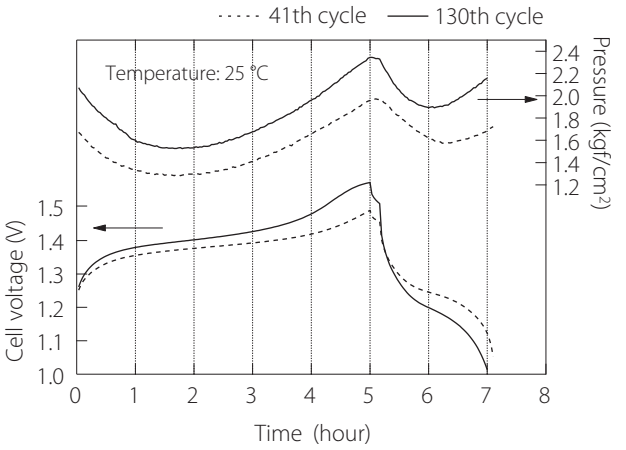

Figure 5: Voltage and pressure observations during charge-discharge process

drastically increased to 10kgf/cm^2 after the 130th cycle. It is considered that the electrode, which absorbs the electrolyte, expands, and therefore, the pressure rose. Electrolyte absorption would cause the separator to dry out, which led to the deterioration of the battery performance.

3.3 Cycle-life performance

Because the polypropylene (PP) nonwoven fabric, which is used as the separator, includes a space between the fibers, the separator thickness can be controlled if it is compressed. Spacers were added as shown in Figure 3 and the separator was compressed so that the design thickness of the separator became 0.2 mm or 0.3 mm when the electrode bundle was placed in the cell frame.

Figure 6 shows the cycle-life performances of the test cell with the design thickness of the separator of 0.2 mm and 0.3 mm. These cells exhibited longer cycle-life than that of the cell in Figure 4. The cycle-life performance of the cell with the 0.2 mm separator was doubled in comparison to that of the cell with the 0.3 mm separator.

The results in Figures 4 and 6 indicate that thinner design thickness gives the longer cycle-life. It is considered that repulsive force from the compressed separator increases pressure to the electrodes, and therefore, the electrolyte absorption by the electrode would be reduced, which maintained the battery performance. Table 3 summarizes the battery performances, such as the discharge voltage and Ah-efficiency. These values were improved with decreasing the separator thickness. Meanwhile, there was a concern that the space decrease due to the separator compression would decrease the electrolyte which could be held in the separator. In order to understand these results, the porosity of the compressed separator was estimated as shown in Figure 7(a). The porosity was equivalent to the ratio of the cavity between the fibers, and it was defined as the shade density of the separator divided by the truth density. The porosity decreased with the increasing compression and became approximately 0 by compressing to 0.1 mm. In addition, the porosity decreased by 10 % when the separator thickness decreased to 0.2 mm from 0.3 mm.

For the measured electrolyte resistivity (R_e = 2 Ω•cm), porosity and separator thickness, the voltage drops were calculated from the following relational expressions.

Resistance between the electrodes (Ω) =
(R_e / porosity (Ω•cm)) × separator thickness (cm) / separator area (cm^2) (1)

Voltage drop during the discharge process (V) =
(1) × discharge current (A) (2)

Figure 7(b) shows the relationship between the separator thickness and discharge-voltage decrease at the 1 C-rate discharge, suggesting that the voltage reduction is slightly de-

Table 3: Sepecification and peformance of the test batteries

Granulated particle electrode		Separator		Battery performance	
Thickness mm	Density g/cm³	Thickness mm	Replusive force kgf/cm²	Average discharge voltage V	Ah efficiency %
1.2	1.9	0.3	< 0.01	1.199	95.3
1.2	1.9	0.2	1.2	1.223	98.2

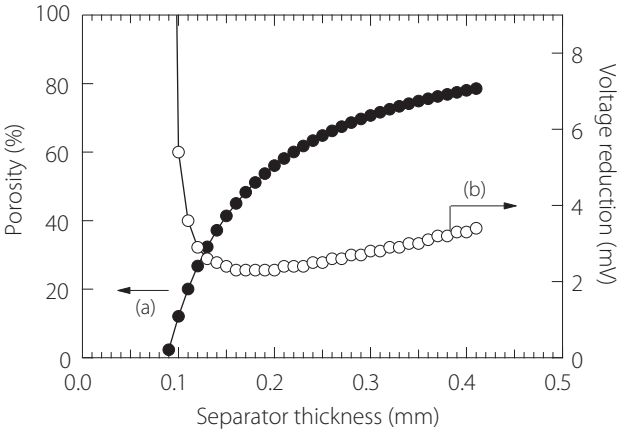

Figure 7: Calculated values of (a) the porosity and (b) voltage drop dependent on the designed separator thickness

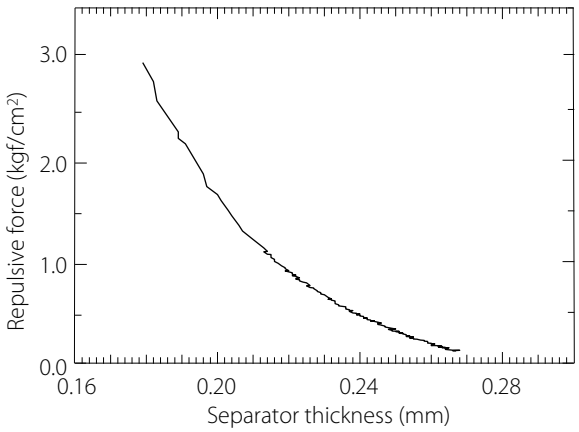

Figure 8: Repulsive force dependent on the compressed separator thickness observed by an autograph instrument

creased when the separator was compressed from 0.3 mm to 0.2 mm. Namely, the porosity decrease in this range does not remove electrolyte from the separator, and there would be little influence on the ionic diffusion during the electrochemical reaction. Meanwhile, the separator compression would increase the adhesion between the active material particle and substrate, and improve the electrical conductivity of the active material. Therefore, at a 0.2 mm separator thickness, the battery performance was improved. This consideration is consistent to the observed voltage value in Table 3. Meanwhile, a high voltage decrease would occur if the electrolyte in the separator could not remain as the porosity approached 0 %. The aim of the compressed separator thickness such that the electrolyte, which does not affect the charge-discharge reaction, would be an approximate 0.15 mm.

Factors affecting the cycle-life improvement for the 0.2 mm separator compression include electrode expansion restraint by the repulsive force from a compressed separator, preventing the electrolyte absorption of the electrode and drying of the separator.

Figure 8 shows the repulsive force of the separator, which was measured by an autograph instrument. The repulsive force was gradually increased when the separator thickness is less than 0.28 mm. A 1.6 kgf/cm^2 repulsive force was observed for the 0.2 mm compressed thickness, while it was approximately 3 kgf/cm^2 at the 0.18 mm. The former value is comparable or higher than that of the observed pressure of the electrode expansion in Figure 5. These results suggest that a moderate repulsive force suppresses the electrode expansion, and contributes to improving the cycle-life performance. A further improvement in the cycle-life performance would be expected by raising the compression to 0.15-0.18 mm.

4. Summary

The active material powder was granulated with ORCB, Ni-CF and EVA, and the granulated particles were sandwiched between two nickel-foam pieces to form plate-like electrodes for the Ni-MH battery. The positive electrode with the 5 wt% of ORCB, Ni-CF and EVA as additives exhibited the highest discharge capacity. The battery test using the GIGACELL-type single cells showed that the cycle-life performance was influenced by the separator compression. At a 0.2 mm separator thickness, no remarkable capacity loss was observed for 2000 cycles. The repulsive force dependent on the separator compression would suppress the electrolyte absorption of the electrode and dry out the separator, contributing to an improved cycle-life performance

References

Falk, S. U. and Salkind, A. J. (1969). *Alkaline Storage Batteries*. John Wiley & Sons.

Fleischer, A. (1948). Sintered plates for nickel-cadmium batteries. *Journal of the Electrochemical Society*, Vol. 94, No. 6, 289-299.

Ng, P. K. and Schneider, W. (1986). Distribution of nickel hydroxide in sintered nickel plaques measured by radiotracer method during electroimpregnation. *Journal of the Electrochemical Society*, Vol. 133, 17-21.

Nishimura, K. and Tsutsumi, K. (2007). A wet synthesis sealing up battery. *Powder Science and Engineering*, Vol. 39, No. 7, 1-6.

Ogura, K., Matsumura, T., Tonda, C., Nishimura, K. and Kataoka, M. (2010). Effective utilization of energy from train regenerative braking: Battery power system for railways. *Kawasaki Technical Review*, Vol. 170, 24-27.

Oshitani, M., Yufu, H., Takashima, K., Tsuji, S. and Matsumaru, Y. (1989). Development of a pasted nickel electrode with high active material utilization. *Journal of the Electrochemical Society*, Vol. 136, 1590-1593.

Sakai, T. (2010). The role of battery technologies for reducing carbon dioxide emission. *Funtai Gijutsu*, Vol. 2, 17-24.

Sakai, T. and Sato, N. (2003). *Development of Large Scale Rechargeable Batteries for Vehicles*. CMC Publishing.

Takasaki, T. and Nishimura, K., Saito, M., Iwaki, T. and Sakai, T. (2013). Cobalt-free materials for nickel-metal hydride battery: self-discharge suppression and overdischarge resistance improvement. *Electrochemistry*, Vol. 81, No. 7, 553-558.

Tsutsumi, K. (2008). The latest energy saving technology development on railway system. *Journal of the Japan Institute of Energy*, Vol. 87, No. 7, 506-509.

Tsutsumi, K. and Matsumura, T. (2009). Revolution in storage battery technology and adoption by electric railways, *Science & Technology in Japan*, Vol. 26, 21-24.

Yamazaki, H., Akiyama, S., Hirashima, T., Kataoka, M. and Matsuo, K. (2010). Urban Transportation that is friendly for people and the environment: SWIMO-X low-floor battery-driven light rail vehicle. *Kawasaki Technical Review*, Vol. 170, 16-19.

Yao, M., Okuno, K., Iwaki, T., Kato, M., Harada, K., Park, J-J., Tanase, S. and Sakai, T. (2007). Influence of nickel foam pore structure on the high-rate capability of nickel/metal-hydride batteries. *Journal of the Electrochemical Society*, Vol. 154, No. 7, A709-A714.

(Received: July 16, 2013; Accepted: August 26, 2013)